AGU PUBLICATIONS

Geophysical Research Letters

RESEARCH LETTER
10.1002/2016GL071579

Key Points:
- Variations in pore water pressure cause dramatic changes in friction against ice flow provided by a subglacial sedimentary bed
- When water pressure varies, sediments creep nonlinearly due to force network reorganization at stress levels below the yield strength
- Sediment strength is limited to the Mohr-Coulomb criterion, which can produce stick-slip behavior in systems with stress oscillations

Supporting Information:
- Supporting Information S1
- Figure S1
- Figure S2
- Data Set S1

Correspondence to:
A. Damsgaard,
adamsgaard@ucsd.edu

Citation:
Damsgaard, A., D. L. Egholm, L. H. Beem, S. Tulaczyk, N. K. Larsen, J. A. Piotrowski, and M. R. Siegfried (2016), Ice flow dynamics forced by water pressure variations in subglacial granular beds, *Geophys. Res. Lett.*, *43*, doi:10.1002/2016GL071579.

Received 12 OCT 2016
Accepted 30 NOV 2016
Accepted article online 5 DEC 2016

Ice flow dynamics forced by water pressure variations in subglacial granular beds

Anders Damsgaard[1,2], David L. Egholm[2], Lucas H. Beem[3], Slawek Tulaczyk[4], Nicolaj K. Larsen[2,5], Jan A. Piotrowski[2], and Matthew R. Siegfried[1]

[1]Institute of Geophysics and Planetary Physics, Scripps Institution of Oceanography, University of California, San Diego, California, USA, [2]Department of Geoscience, Aarhus University, Aarhus, Denmark, [3]Institute for Geophysics, University of Texas, Austin, Texas, USA, [4]Department of Earth and Planetary Sciences, University of California, Santa Cruz, California, USA, [5]Centre for GeoGenetics, Natural History Museum of Denmark, University of Copenhagen, Copenhagen, Denmark

Abstract Glaciers and ice streams can move by deforming underlying water-saturated sediments, and the nonlinear mechanics of these materials are often invoked as the main reason for initiation, persistence, and shutdown of fast-flowing ice streams. Existing models have failed to fully explain the internal mechanical processes driving transitions from stability to slip. We performed computational experiments that show how rearrangements of load-bearing force chains within the granular sediments drive the mechanical transitions. Cyclic variations in pore water pressure give rise to rate-dependent creeping motion at stress levels below the point of failure, while disruption of the force chain network induces fast rate-independent flow above it. This finding contrasts previous descriptions of subglacial sediment mechanics, which either assume rate dependence regardless of mechanical state or unconditional stability before the sediment yield point. Our new micromechanical computational approach is capable of reproducing important transitions between these two end-member models and can explain multimodal velocity patterns observed in glaciers, landslides, and slow-moving tremor zones.

1. Introduction

Glaciers and ice sheets flow by three main mechanisms [*Cuffey and Paterson*, 2010]: (1) viscous deformation of ice, (2) sliding at the ice bed interface, and (3) deformation of subglacial sediments [*Iverson et al.*, 1995; *Hooke et al.*, 1997; *Tulaczyk et al.*, 2000]. Fast flow occurs where the ice base is at the pressure melting point, which is governed by the weight of the overlying ice, heat dissipation accompanying sliding and deformation, latent heat, and geothermal flux. Such thermal conditions allow liquid water in the subglacial environment. Hence, sedimentary subglacial beds often host melt water saturated and actively deforming granular materials (till), consisting of either reworked older sedimentary deposits or mobilized products from glacial erosion [*Cuffey and Paterson*, 2010; *Stokes et al.*, 2016]. Till may become weaker than glacier ice when water pressure is high, because the frictional failure strength of sediments is controlled by effective stress (i.e., the difference between total load and pore water pressure). Till deformation may be the main driver of glacier flow under these conditions [*Hooke et al.*, 1997; *Cuffey and Paterson*, 2010], and fast ice flow is often collocated with sedimentary beds [*Anandakrishnan et al.*, 1998; *Tulaczyk et al.*, 2000; *Peters et al.*, 2006].

The mechanical behavior of subglacial till is thus of primary importance to the motion of glaciers and ice sheets. However, the grain-scale controls on till strength and deformation style are poorly known. The subglacial environment is difficult to access and experimentally analyze, and the physics of subglacial till deformation has consequently been a topic of long-lasting and intense discussion [e.g., *Alley et al.*, 1986; *Boulton and Hindmarsh*, 1987; *Kamb*, 1991; *Iverson et al.*, 1995; *Hooke et al.*, 1997; *Iverson et al.*, 1998; *Tulaczyk et al.*, 2000; *Fowler*, 2003; *Rathbun et al.*, 2008; *Damsgaard et al.*, 2013, 2015]. The constitutive relations proposed for till range from nearly linear viscous [*Alley et al.*, 1986; *Boulton and Hindmarsh*, 1987; *Alley et al.*, 1987] to frictional with slight velocity strengthening [*Hooke et al.*, 1997; *Kamb*, 1991; *Tulaczyk et al.*, 2000; *Tulaczyk*, 2006] or weakening [*Iverson et al.*, 1998; *Iverson and Zoet*, 2015]. A nearly linear viscous till would strongly dampen variations in ice flow velocity by increasing or decreasing basal resistance when ice motion accelerates or decelerates, respectively. Models based on plasticity and friction, on the other hand, predict till strength with little or no velocity dependence, and they can explain rapid flow oscillations and unstable feedbacks in glacier flow, which may ultimately lead to ice sheet reorganization or collapse [*Kamb*, 1991; *Parizek et al.*, 2013; *Bougamont et al.*, 2015; *Ritz et al.*, 2015]. Evidence from in situ measurements and laboratory

experiments strongly supports the latter type of models with little correlation between glacier sliding velocity and subglacial till strength. The strength seems instead to be controlled by effective stress, the fraction of ice overburden that is not carried by subglacial water pressure [*Hooke et al*., 1997; *Fischer and Clarke*, 1997; *Kamb*, 1991; *Iverson et al*., 1998; *Tulaczyk et al*., 2000; *Damsgaard et al*., 2013, 2015].

The influence of effective stress on glacier flow over sedimentary and bedrock beds is supported by several studies showing a positive correlation between surface melt production, subglacial water pressure, and glacier velocity [e.g., *Hooke et al*., 1997; *Fischer and Clarke*, 1997; *Bartholomaus et al*., 2008; *Andrews et al*., 2014]. Glaciers can accelerate when melt water produced at the surface is routed to the glacier bed, causing water pressure to increase. Likewise, many West Antarctic ice streams that drain ice to the ocean flow at highly variable speeds, because tidal movements in the floating part of the glacier modulate the upstream distribution of pore water pressure and stress from the ice [e.g., *Bindschadler et al*., 2003; *Winberry et al*., 2011; *Walker et al*., 2013; *Thompson et al*., 2014; *Rosier et al*., 2015]. Although surface-melting glaciers and Antarctic tidal ice streams are dissimilar in many ways, the basic reason for their variable velocity may be similar: reduction of effective stress weakens the frictional strength of the glacier bed. The impact of effective stress on steady state till rheology has been previously considered [*Kamb*, 1991; *Hooke et al*., 1997; *Fischer and Clarke*, 1997; *Iverson et al*., 1998; *Tulaczyk et al*., 2000; *Iverson and Iverson*, 2001; *Damsgaard et al*., 2013, 2015] but not the impact of water pressure fluctuations on micromechanical granular stability before and during plastic failure.

2. Methods

In order to study the mechanical response of a granular bed to transient stress perturbations, we designed computational experiments where the force balance of a fluid-saturated granular material is disturbed by variations in effective stress normal to the granular bed (Figure 1). The grains and fluid are simulated using two separate but coupled numerical algorithms, implemented for GPU computing [*NVIDIA*, 2015]. The granular phase is approximated by the soft-body discrete element method with elastic frictional contacts [*Cundall and Strack*, 1979; *Hinrichsen and Wolf*, 2004; *Luding*, 2008; *Kruggel-Emden et al*., 2008; *Radjaï and Dubois*, 2011; *Damsgaard et al*., 2013] and is fully two-way coupled to the fluid phase with water pressures evolving according to changes in porosity and Darcian porous flow [*McNamara et al*., 2000; *Zhou et al*., 2010; *Goren et al*., 2010, 2011; *Damsgaard et al*., 2015]. The local hydraulic permeability is scaled by local porosity [*Hazen*, 1910; *Kozeny*, 1927; *Carman*, 1937; *Harleman et al*., 1963; *McNamara et al*., 2000; *Goren et al*., 2011; *Damsgaard et al*., 2015]. The computational experiment involves a small three-dimensional sample ($0.52 \times 0.26 \times 0.55$ m) of sediment represented by 9600 spherical grains of uniform size. The lower boundary is static and impermeable, while a flat and mobile upper wall exerts a defined and time variable normal stress downward onto the granular assemblage. Fluid pressure is adjusted accordingly in the cells containing the upper wall. Fluid mass is conserved everywhere in the domain, with the exception of the uppermost cells with a prescribed water pressure, similar to "drained" geotechnical laboratory setups [e.g., *Bowles*, 1992]. Lateral boundaries are periodic for both the granular and fluid phases. Prior to the shear experiment, the grains are consolidated under uniaxial compression. A constant shear stress applied to the uppermost layer of grains induces shear movement. Simulation parameters are listed in Table S1 in the supporting information. An extended description of methods is available in Text S1 and references therein. The comparability between experiment and true subglacial setting thus relies on the scale independency of granular geotechnical properties [*Fowler*, 2003; *Tulaczyk*, 2006], and the fundamental consistency of the Mohr-Coulomb failure envelope across different materials and grain sizes. The model is not designed to reproduce the ductile behavior of very clay-rich materials.

This approach is new for a subglacial setting but highly rewarding compared to standard continuum methods (i.e., the viscous and plastic models mentioned above), because it obviates a priori assumptions regarding the macroscopic rate dependency of the material strength. Generally speaking, the mechanical behavior of a granular material results from the properties of the individual grains and their collective self-organizing arrangement. Transitions in the mechanical state of granular materials are known to drastically influence the load-bearing capacity [e.g., *Jaeger and Nagel*, 1992].

The external forcings, namely, shear stress and pore water pressure, were calibrated to mimic subglacial conditions where water pressure may vary at considerably shorter time scales than shear stress. The shear stress was thus held constant at 10 kPa, while pore water pressure at the top of the bed was prescribed to oscillate

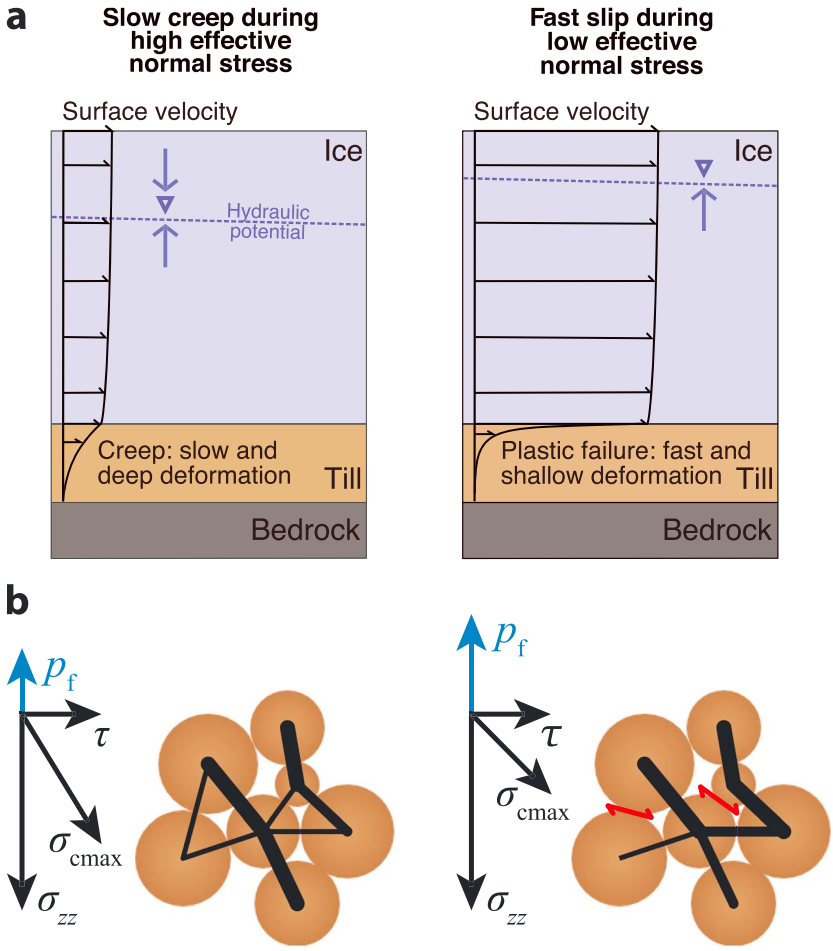

Figure 1. Schematic representation of ice flow and granular deformation in the glacier bed. (a) The granular till bed (left) slowly creeps due to variations in pore water pressure or (right) slips rapidly due to yield failure. Figure is not to scale. (b) Variations in pore water pressure (p_f) modify the direction and magnitude of the maximum compressive strength (σ_{cmax}) in the sedimentary bed. The black lines represent the granular stress and the red arrows denote contact sliding. At lower p_f (left diagram in Figure 1b) grain contact friction inhibits deformation. At higher p_f (right diagram in Figure 1b) grains can slide past each other as internal stresses change over time. The cumulative deformation contributed by grain-scale slip events leads to local reorganization of the granular force network and creeping motion beneath the yield stress and unconstrained bed acceleration at greater driving stresses.

with a diurnal amplitude of 70 kPa, causing changes in effective normal stress around a mean value of 80 kPa (Figure 2a). Plastic failure is known to occur in this simulated material when the magnitude of applied shear stress equals 30% of the effective normal stress or more [*Damsgaard et al.*, 2013, 2015]. All parts of the granular assemblage were free to move and accelerate at any rate dictated by the net force and torque on each grain.

3. Stick, Creep, and Slip

In our experiments, the granular bed showed highly nonlinear velocity variations in response to the fluctuating effective pressure. Periods of minimum motion—stick events, when static force chains caused jamming and a solid-like rigidity of the granular assemblage—were possible during times of maximum effective normal stress and low variation in pore water pressure. In contrast, periods of slip, with rapid deformation of a thin boundary layer of grains, occurred when effective normal stress was lowered enough to push the macroscopic yield strength below the externally imposed shear stress. Moreover, a key finding of our experiments was that the granular material showed creep in the periods between the stick-slip phases with velocities between 10^{-8} and 10^{-6} m/s (Figure 2b and Figure S1 in the supporting information). The rate of creep

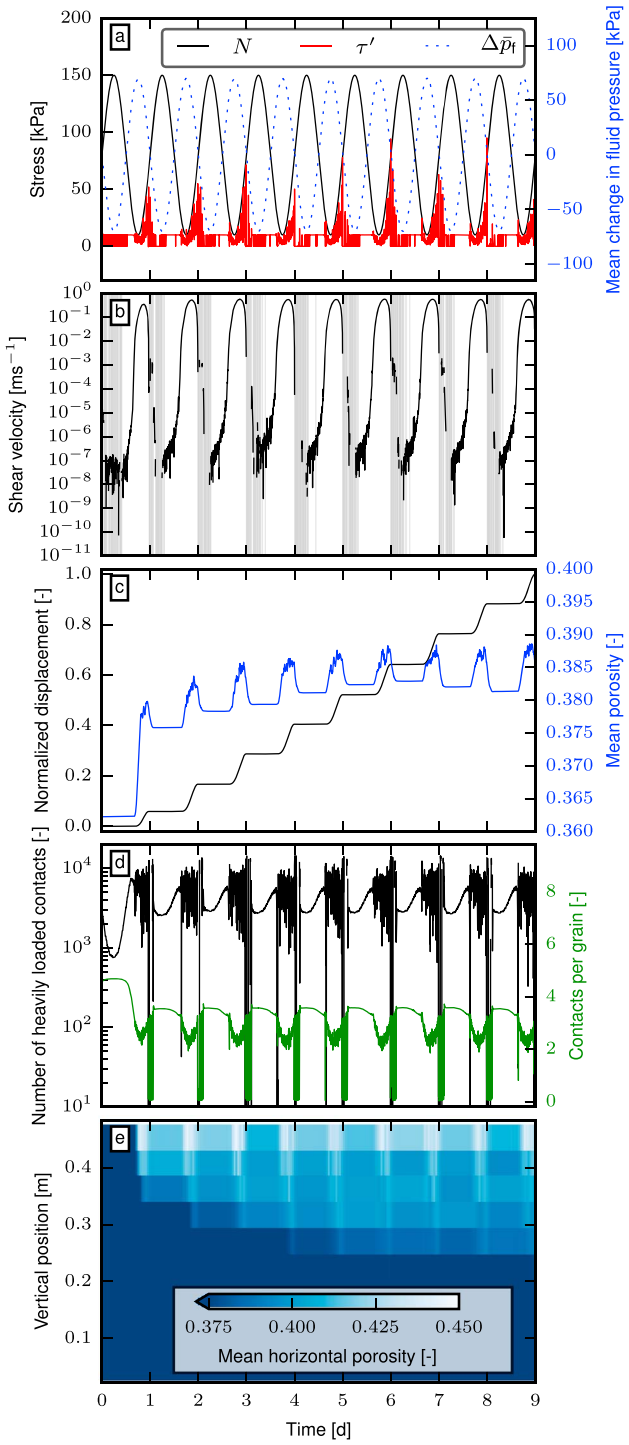

Figure 2. Granular dynamics in computational experiments forced by cyclic variation of water pressure. (a) Cyclic modulation of pore water pressure (Δp_f; blue, right axis) at the upper boundary affects effective normal stress (N; black, left axis) and changes the ratio between shear stress (τ'; red, left axis) and the effective normal stress (N). The large values of recorded shear stress occur when the material slows down after runaway failure. (b) The stability of the granular assemblage is determined by the τ'/N ratio, and the material responds by (1) stick during low and decreasing τ'/N ratios (gray vertical bars), (2) slow creep for low and increasing τ'/N ratios, or (3) slip during high τ'/N ratios. (c) The irregular velocity pattern results in a stepwise displacement, where mean porosities are constant during creep and elevated during fast slip. (d) The number of relatively heavily loaded grain pairs increases as the effective normal stress decreases, while the mean number of contacts per particle decreases. (e) The internal porosity increases in areas of active deformation, which become deeper over the course of several cycles.

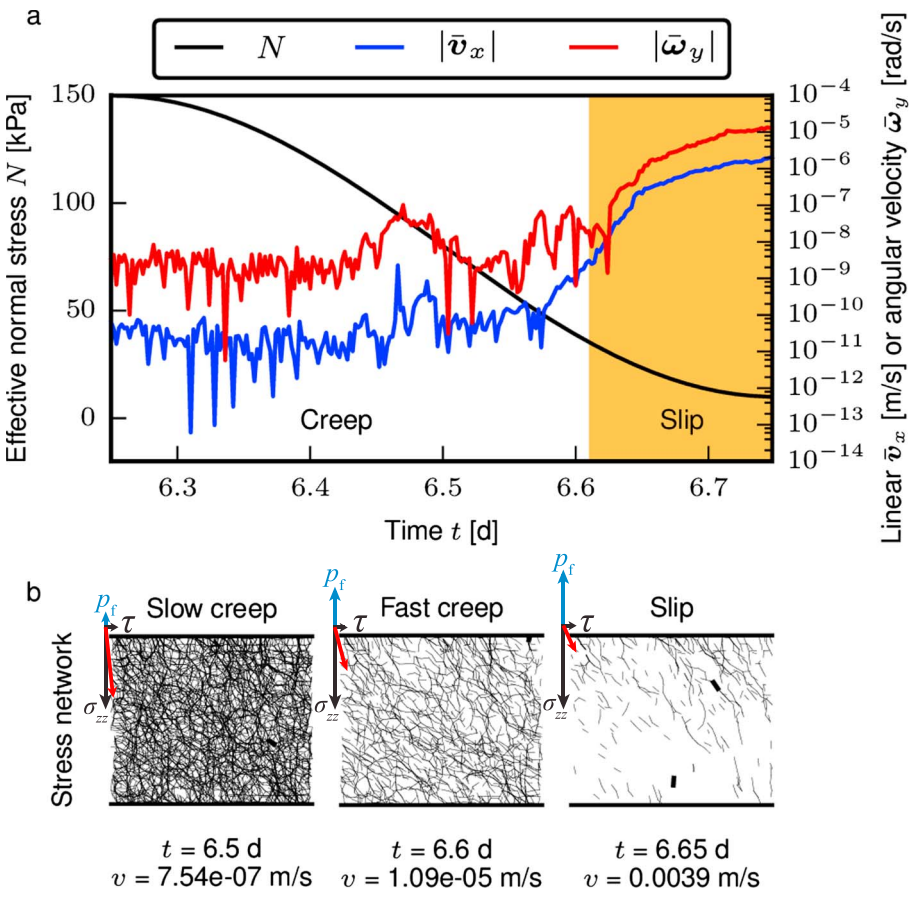

Figure 3. Granular dynamics in response to decreasing effective normal stress. (a) Effective normal stress (black) and averaged grain movement (linear: blue; angular: red). Grain rearrangement accelerates nonlinearly as effective normal stress decreases. The shear velocity contributed by grain rolling is less than the grain linear displacement when converting angular velocity to grain surface displacement rate. (b) Internal distribution of stress between grains (black lines) at different stages of the granular flow. The granular contact stress is mainly in the direction of the applied principal stress represented by the red arrow.

decayed rapidly under constant-stress forcing, but repeated variations in effective normal stress caused the orientation and magnitude of the maximum compressive stress to change correspondingly. These changes required the grains to geometrically reorganize in order to obtain a packing capable of supporting the new orientation of the principal stress (Figure 1b). The grains responded by small-scale deformation by intergrain contact sliding and reorientation when the contacts were unfavorably oriented relative to the principal stress. The contact reorganization caused relatively large creep velocities and a high level of porosity in the sediment, and the material did not consolidate to prefailure packing under maximum effective normal stress (Figures 2c and 2e). The creep was caused by distributed deformation contrary to the shallow deformation during slip failure.

The finding of prefailure creep in idealized granular materials contrasts with the perfectly plastic material rheology, where no deformation occurs at stress levels below the yield strength. The combination of creep and stick-slip results in a stepped displacement history (Figure 2c). Creep has for a long time been recognized as a deformation mode preceding plastic failure [e.g., *Griggs*, 1936; *Terzaghi*, 1950], but the governing processes are poorly constrained. Creep rates in geotechnical materials subjected to a constant deviatoric stress just below its ultimate failure strength are known to decay logarithmically with time [e.g., *Kamb*, 1991; *Moore and Iverson*, 2002; *Nguyen et al*., 2011] or to lead to runaway failure [e.g., *Mitchell and Soga*, 2006]. Our experiments suggest that repeated perturbation of effective stress causes sustained internal grain rearrangement (Figure 3), which has also recently been observed in laboratory experiments on simple granular materials

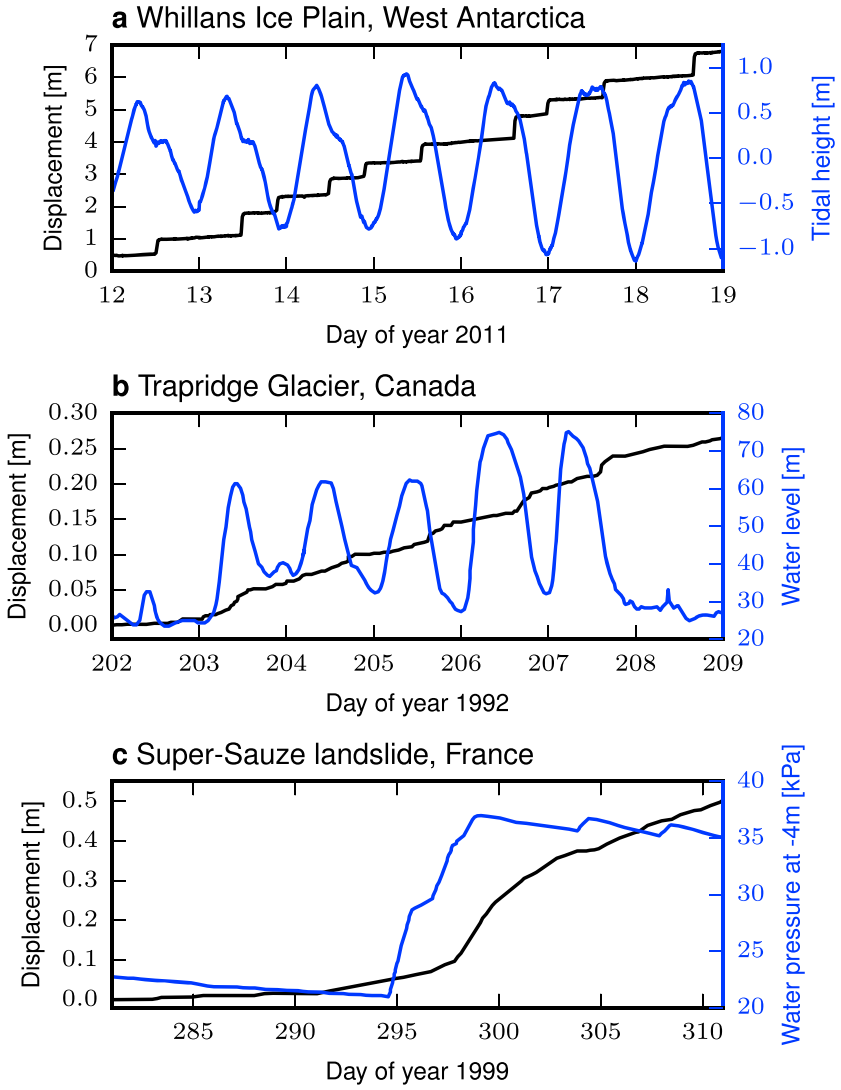

Figure 4. (a, b) Creep and slip due to pore pressure variation in two glacial systems and (c) an active landslide. All three systems display slow but measurable displacement during periods of low but variable water pressure, corresponding to the creep in our numerical simulations (Figure 2b). Trapridge Glacier data from *Fischer and Clarke* [1997], Super-Sauze landslide data from *Malet et al.* [2002].

[*Pons et al.*, 2015]. This behavior is analogous to how granular materials on hillslopes beneath the angle of repose experience downslope movement due to episodic disturbances, e.g., wet-dry or freeze-thaw cycles [*Roering et al.*, 2001]. The flow of slow-moving landslides is sensitive to transient stress perturbations such as variations in pore water pressure by discrete precipitation events [*Roering et al.*, 2001] or variations in atmospheric pressure [*Schulz et al.*, 2009]. Similarly, continued creep is observed in water flow-driven sediment transport [*Houssais et al.*, 2015; *Houssais and Jerolmack*, 2016]. Processes such as fluid migration or the arrival of teleseismic waves can disturb the balance of stresses in earthquake faults and are hypothesized to cause slow-slip tremor episodes or initiate fast slip accompanying earthquakes [*Schwartz and Rokosky*, 2007; *Shelly et al.*, 2011; *Peng et al.*, 2014]. We expect creep to dominate bulk shear strain if the yield strength is not exceeded at all, or if the duration of plastic failure is relatively short. Creep is most significant when the material is stressed just below the yield strength due to the strong observed nonlinearity between driving stresses and the resultant shear strain rate (Figure S1 in the supporting information).

We compared our model results to observations from a mountain glacier, an ice stream, and a landslide, which are all phenomena in which deformation of granular materials plays an important role (Figure 4).

The variations in water pressure have in these settings and in our experiment very different amplitudes. However, from our results we expect that smaller water pressure variations are needed in systems with low effective normal stress, and vice versa. At Whillans Ice Plain, West Antarctica, tidal variations induce flow oscillation (Figures 4a and S2) [*Bindschadler et al*., 2003; *Winberry et al*., 2011] and Trapridge Glacier in Canada shows similar displacement when surface melt drains through crevasses to the sedimentary bed, causing periodic ice bed decoupling during drainage and slow movement at low subglacial water pressure (Figure 4b) [*Fischer and Clarke*, 1997]. The flow of the Super-Sauze landslide in France (Figure 4c) is strongly linked to discrete precipitation events that alter the internal water level [*Malet et al*., 2002]. In all three settings nonlinear granular dynamics causes flow to switch between fast slip and slow creep. The slip phases correspond to plastic failure of the granular bed when water pressure exceeds a threshold value. Slow flow between slips may be caused by elastic loading, viscoelastic ice deformation, basal sliding in the glacial systems, and the granular creep mechanism presented here. While diurnal-scale variations in pore water pressure drive the granular creep, longer-term changes in mean water pressure set the pace of the creep and influence the duration of slip events [*Beem et al*., 2014; *Winberry et al*., 2014; *Siegfried et al*., 2016]. The creep in our experiments is caused by distributed deformation, while slip is accommodated by shallow deformation. This difference in deformational depth may explain the discrepancy between seismic and in situ investigations of deforming bed thicknesses [e.g., *Blankenship et al*., 1986; *Engelhardt et al*., 1990].

4. Summary

Shear deformation of subglacial sediments contributes significantly to ice stream flow in many cases. On diurnal time scales, variations in subglacial water pressure and driving stress can cause stick-slip movement [e.g., *Rosier et al*., 2015], while on time scales of centuries, the same variations can cause ice stream shutdown and initiation [e.g., *Bougamont et al*., 2015]. From two-phase computational experiments we demonstrated that stick due to granular jamming is rare, as changes in the deviatoric stress cause grain contact failures leading to prefailure creep that can be fitted with a nonlinear rate-dependent relationship. Above the yield strength the rheology becomes rate independent. Creep will dominate the bulk shear strain if the yield strength is not exceeded, if the duration of plastic failure is short, and/or if driving stresses are close to the yield strength. The extreme sensitivity of granular flow to changes in shear stress or water pressure highlights the importance of understanding the coupled mechanics of stick-slip and creep in a wide range of natural environments. Our micromechanical computational approach offers a solution to explain the observed multimodal velocity patterns in fast moving ice streams, landslides, and tectonic faults by a combination of stick-slip and creep in granular materials.

Acknowledgments
This work was supported by the Danish Council for Independent Research under the Sapere Aude program and the Cecil H. and Ida M. Green Foundation. GPS data collection from the Whillans Ice Plain was supported by NSF grants (ANT-0838885, ANT-0839142, and ANT-0636970) as part of the interdisciplinary WISSARD project. Applied software and simulation scripts are available from https://github.com/anders-dc/sphere. The presented GPS record data are available in the supporting information (Data File S1). We thank Poul Christoffersen, Martin Truffer, and Morgane Houssais for helpful discussion and appreciate the constructive comments by Roger LeB. Hooke and an anonymous reviewer. The authors declare no financial conflicts of interests.

References

Abe, S., and K. Mair (2005), Grain fracture in 3D numerical simulations of granular shear, *Geophys. Res. Lett.*, *32*, L05305, doi:10.1029/2004GL022123.

Aharonov, E., and D. Sparks (1999), Rigidity phase transition in granular packings, *Phys. Rev. E*, *60*, 6890–6896, doi:10.1103/PhysRevE.60.6890.

Aharonov, E., and D. Sparks (2002), Shear profiles and localization in simulations of granular shear, *Phys. Rev. E*, *65*, 051302, doi:10.1103/PhysRevE.65.051302.

Alley, R. B., and I. M. Whillans (1991), Changes in the West Antarctic ice sheet, *Science*, *254*, 959–963, doi:10.1126/science.254.5034.959.

Alley, R. B., D. D. Blankenship, C. R. Bentley, and S. T. Rooney (1986), Deformation of till beneath ice stream B, West Antarctica, *Nature*, *322*, 57–59, doi:10.1038/322057a0.

Alley, R. B., D. D. Blankenship, S. T. Rooney, and C. R. Bentley (1987), Till beneath ice stream B 4. A coupled ice-till flow model, *J. Geophys. Res.*, *92*, 8931–8940, doi:10.1029/JB092iB09p08931.

Anandakrishnan, S., D. D. Blankenship, R. B. Alley, and P. L. Stoffa (1998), Influence of subglacial geology on the position of a West Antarctic ice stream from seismic observations, *Nature*, *394*, 62–65, doi:10.1038/27889.

Andrews, L. C., G. A. Catania, M. J. Hoffman, J. D. Gulley, M. P. Lüthi, C. Ryser, R. L. Hawley, and T. A. Neumann (2014), Direct observations of evolving subglacial drainage beneath the Greenland Ice Sheet, *Nature*, *514*, 80–83, doi:10.1038/nature13796.

Bartholomaus, T. C., R. S. Anderson, and S. P. Anderson (2008), Response of glacier basal motion to transient water storage, *Nat. Geosci.*, *1*, 33–37, doi:10.1038/ngeo.2007.52.

Beem, L. H., S. M. Tulaczyk, M. A. King, M. Bougamont, H. A. Fricker, and P. Christoffersen (2014), Variable deceleration of Whillans Ice Stream, West Antarctica, *J. Geophys. Res. Earth Surf.*, *119*, 212–224, doi:10.1002/2013JF002958.

Bindschadler, R. A., M. A. King, R. B. Alley, S. Anandakrishnan, and L. Padman (2003), Tidally controlled stick-slip discharge of a West Antarctic ice stream, *Science*, *301*, 1087–1089, doi:10.1126/science.1087231.

Blankenship, D. D., C. R. Bentley, S. T. Rooney, and R. B. Alley (1986), Seismic measurements reveal a saturated porous layer beneath an active Antarctic ice stream, *Nature*, *322*, 54–57, doi:10.1038/322054a0.

Bougamont, M., P. Christoffersen, S. F. Price, H. A. Fricker, S. Tulaczyk, and S. P. Carter (2015), Reactivation of Kamb Ice Stream triggers century-scale reorganization of Siple Coast ice flow in West Antarctica, *Geophys. Res. Lett.*, *42*, 8471–8480, doi:10.1002/2015GL065782.

Boulton, G. S., and R. C. A. Hindmarsh (1987), Sediment deformation beneath glaciers: Rheology and geological consequences, *J. Geophys. Res.*, *92*, 9059–9082, doi:10.1029/JB092iB09p09059.
Bowles, J. E. (1992), *Engineering Properties of Soils and Their Measurement*, McGraw-Hill, New York.
Campbell, C. S. (2006), Granular material flows—An overview, *Powder Technol.*, *162*, 208–229, doi:10.1016/j.powtec.2005.12.008.
Carman, P. C. (1937), Fluid flow through granular beds, *Trans. Inst. Chem. Eng. London*, *15*, 150–166.
Cuffey, K. M., and W. S. B. Paterson (2010), *The Physics of Glaciers*, Academic Press, Amsterdam, doi:10.1016/B978-0-12-369461-4.00001-6.
Cundall, P. A., and O. D. L. Strack (1979), A discrete numerical model for granular assemblies, *Geotechnique*, *29*(1), 45–65, doi:10.1680/geot.1979.29.1.47.
Damsgaard, A., D. L. Egholm, J. A. Piotrowski, S. Tulaczyk, N. K. Larsen, and K. Tylmann (2013), Discrete element modeling of subglacial sediment deformation, *J. Geophys. Res. Earth Surf.*, *118*, 2230–2242, doi:10.1002/2013JF002830.
Damsgaard, A., D. L. Egholm, J. A. Piotrowski, S. Tulaczyk, N. K. Larsen, and C. F. Brædstrup (2015), A new methodology to simulate subglacial deformation of water-saturated granular material, *Cryosphere*, *9*, 2183–2200, doi:10.5194/tc-9-2183-2015.
Engelhardt, H., N. Humphrey, B. Kamb, and M. Fahnestock (1990), Physical conditions at the base of a fast moving Antarctic ice stream, *Science*, *248*, 57–59, doi:10.1126/science.248.4951.57.
Ferziger, J. H., and M. Perić (2002), *Computational Methods for Fluid Dynamics*, Springer, Berlin, doi:10.1007/978-3-642-56026-2.
Fischer, U. H., and G. K. C. Clarke (1997), Stick-slip sliding behaviour at the base of a glacier, *Ann. Glaciol.*, *24*, 390–396.
Fowler, A. C. (2003), On the rheology of till, *Ann. Glaciol.*, *37*, 55–59, doi:10.3189/172756403781815951.
GDR-MiDi (2004), On dense granular flows, *Eur. Phys. E*, *14*, 341–365, doi:10.1140/epje/i2003-10153-0.
Goren, L., E. Aharonov, D. Sparks, and R. Toussaint (2010), Pore pressure evolution in deforming granular material: A general formulation and the infinitely stiff approximation, *J. Geophys. Res.*, *115*, B09216, doi:10.1029/2009JB007191.
Goren, L., E. Aharonov, D. Sparks, and R. Toussaint (2011), The mechanical coupling of fluid-filled granular material under shear, *Pure Appl. Geophys.*, *168*(12), 2289–2323, doi:10.1007/s00024-011-0320-4.
Griggs, D. T. (1936), Deformation of rocks under high confining pressures: I. Experiments at room temperature, *J. Geol.*, *44*, 541–577, doi:10.1086/624455.
Harleman, D. R. F., P. F. Mehlhorn, and R. R. Rumer (1963), Dispersion-permeability correlation in porous media, *J. Hydraul. Div., Am. Soc. Civ. Eng.*, *89*, 67–85.
Hazen, A. (1910), Discussion of dams on sand formation, *Trans. Am. Soc. Civ. Eng.*, *73*, 119–221.
Hinrichsen, H., and D. E. Wolf (2004), *The Physics of Granular Media*, Wiley, Hoboken, N. J., doi:10.1002/352760362X.
Hooke, R. L. B., and N. R. Iverson (1995), Grain-size distribution in deforming subglacial tills: Role of grain fracture, *Geology*, *23*, 57–60, doi:10.1130/0091-7613(1995)023<0057:GSDIDS>2.3.CO;2.
Hooke, R. L. B., B. Hanson, N. R. Iverson, P. Jansson, and U. H. Fischer (1997), Rheology of till beneath Storglaciären, Sweden, *J. Glaciol.*, *43*(143), 172–179, doi:10.3198/1997JoG43-143-172-179.
Houssais, M., and D. J. Jerolmack (2016), Toward a unifying constitutive relation for sediment transport across environments, *Geomorphology*, *277*, 251–264, doi:10.1016/j.geomorph.2016.03.026.
Houssais, M., C. P. Ortiz, D. J. Durian, and D. J. Jerolmack (2015), Onset of sediment transport is a continuous transition driven by fluid shear and granular creep, *Nat. Commun.*, *6*, 6527, doi:10.1038/ncomms7527.
Iverson, N. R., and R. M. Iverson (2001), Distributed shear of subglacial till due to Coulomb slip, *J. Glaciol.*, *47*, 481–488, doi:10.3189/172756501781832115.
Iverson, N. R., and L. K. Zoet (2015), Experiments on the dynamics and sedimentary products of glacier slip, *Geomorphology*, *244*, 121–134, doi:10.1016/j.geomorph.2015.03.027.
Iverson, N. R., B. Hanson, R. L. B. Hooke, and P. Jansson (1995), Flow mechanism of glaciers on soft beds, *Science*, *267*, 80–81, doi:10.1126/science.267.5194.80.
Iverson, N. R., T. S. Hooyer, and R. W. Baker (1998), Ring-shear studies of till deformation: Coulomb-plastic behavior and distributed strain in glacier beds, *J. Glaciol.*, *148*, 634–642, doi:10.3198/1998JoG44-148-634-642.
Jaeger, H. M., and S. R. Nagel (1992), Physics of the granular state, *Science*, *255*, 1523–1531, doi:10.1126/science.255.5051.1523.
Kamb, B. (1991), Rheological nonlinearity and flow instability in the deforming bed mechanism of ice stream motion, *J. Geophys. Res.*, *96*, 16,585–16,595, doi:10.1029/91JB00946.
Kozeny, J. (1927), Ueber kapillare leitung des wassers im boden, *Sitzber. Akad. Wiss. Wien*, *136*, 271–306.
Krimer, D. O., S. Mahle, and M. Liu (2012), Dip of the granular shear stress, *Phys. Rev. E*, *82*, 061312, doi:10.1103/PhysRevE.86.061312.
Kruggel-Emden, H., M. Sturm, S. Wirtz, and V. Scherer (2008), Selection of an appropriate time integration scheme for the discrete element method (DEM), *Comput. Chem. Eng.*, *32*, 2263–2279, doi:10.1016/j.compchemeng.2007.11.002.
Luding, S. (2008), Introduction to discrete element methods: Basic of contact force models and how to perform the micro-macro transition to continuum theory, *Eur. J. Environ. Civ. Eng.*, *12*(7–8), 785–826, doi:10.1080/19648189.2008.9693050.
Mair, K., K. M. Frye, and C. Marone (2002), Influence of grain characteristics on the friction of granular shear zones, *J. Geophys. Res.*, *107*(B10), 2219, doi:10.1029/2001/JB000516.
Malet, J.-P., O. Maquaire, and E. Calais (2002), The use of global positioning system techniques for the continuous monitoring of landslides: Application to the Super-Sauze earthflow (Alpes-de-Haute-Provence, France), *Geomorphology*, *43*(1–2), 33–54, doi:10.1016/S0169-555X(01)00098-8.
McNamara, S., E. G. Flekkøy, and K. J. Måløy (2000), Grains and gas flow: Molecular dynamics with hydrodynamic interactions, *Phys. Rev. E*, *61*(4), 4054–4059, doi:10.1103/PhysRevE.61.4054.
Mitchell, J. K., and K. Soga (2006), *Fundamentals of Soil Behavior*, Wiley, New York.
Moore, P. L., and N. R. Iverson (2002), Slow episodic shear of granular materials regulated by dilatant strengthening, *Geology*, *30*, 843–846, doi:10.1130/0091-7613(2002)030<0843:SESOGM>2.0.CO;2.
Nguyen, V. B., T. Darnige, A. Bruand, and E. Clement (2011), Creep and fluidity of a real granular packing near jamming, *Phys. Rev. Lett.*, *107*, 138303, doi:10.1103/PhysRevLett.107.138303.
NVIDIA (2015), CUDA C Programming Guide, NVIDIA Corporation, Santa Clara, Calif. [Available at http://docs.nvidia.com/cuda/cuda-c-programming-guide/index.html.]
Parizek, B. R., et al. (2013), Dynamic (in)stability of Thwaites Glacier, West Antarctica, *J. Geophys. Res. Earth Surf.*, *118*, 638–655, doi:10.1002/jgrf.20044.
Patankar, S. V. (1980), *Numerical Heat Transfer and Fluid Flow*, CRC Press, Boca Raton, Fla.
Peng, Z., J. I. Walter, R. C. Aster, A. Nyblade, D. A. Wiens, and S. Anandakrishnan (2014), Antarctic icequakes triggered by the 2010 Maule earthquake in Chile, *Nat. Geosci.*, *7*, 677–681, doi:10.1038/ngeo2212.

Peters, L. E., S. Anandakrishnan, R. B. Alley, J. P. Winberry, D. E. Voigt, A. M. Smith, and D. L. Morse (2006), Subglacial sediments as a control on the onset and location of two Siple Coast ice streams, West Antarctica, *J. Geophys. Res.*, *111*, B01302, doi:10.1029/2005JB003766.

Pons, A., A. Amon, T. Darnige, J. Crassous, and E. Clément (2015), Mechanical fluctuations suppress the threshold of soft-glassy solids: The secular drift scenario, *Phys. Rev. E*, *92*, 020201, doi:10.1103/PhysRevE.92.020201.

Press, W. H., S. A. Teukolsky, W. T. Vetterling, and B. P. Flannery (2007), *Numerical Recipes*, *The Art of Sci. Comput*., 3rd ed., Cambridge Univ. Press, Cambridge, U. K.

Radjaï, F., and F. Dubois (2011), *Discrete-Element Modeling of Granular Materials*, ISTE-Wiley, London, U. K.

Rathbun, A. P., C. Marone, R. B. Alley, and S. Anandakrishnan (2008), Laboratory study of the frictional rheology of sheared till, *J. Geophys. Res.*, *113*, F02020, doi:10.1029/2007JF000815.

Rignot, E. J., J. Mouginot, and B. Scheuchl (2011), Ice flow of the Antarctic Ice Sheet, *Science*, *333*, 1427–1430, doi:10.1126/science.1208336.

Ritz, C., T. E. Edwards, G. Durand, A. J. Payne, V. Peyaud, and R. C. A. Hindmarsh (2015), Potential sea-level rise from Antarctic ice-sheet instability constrained by observations, *Nature*, *528*, 115–118, doi:10.1038/nature16147.

Roering, J. J., J. W. Kirchner, L. S. Sklar, and W. E. Dietrich (2001), Hillslope evolution by nonlinear creep and landsliding: An experimental study, *Geology*, *29*, 143–146, doi:10.1130/0091-7613(2001)029<0143:HEBNCA>2.0.CO;2.

Rosier, S. H. R., G. H. Gudmundsson, and J. A. M. Green (2015), Temporal variations in the flow of a large Antarctic ice stream controlled by tidally induced changes in the subglacial water system, *Cryosphere*, *9*, 1649–1661, doi:10.5194/tc-9-1649-2015.

Schulz, W. H., J. W. Kean, and G. Wang (2009), Landslide movement in southwest Colorado triggered by atmospheric tides, *Nat. Geosci.*, *2*, 863–866, doi:10.1038/ngeo659.

Schwartz, S. Y., and J. M. Rokosky (2007), Slow slip events and seismic tremor at circum-Pacific subduction zones, *Rev. Geophys.*, *45*, RG3004, doi:10.1029/2006RG000208.

Shelly, D. R., Z. Peng, D. H. Hill, and C. Aiken (2011), Triggered creep as a possible mechanism for delayed dynamic triggering of tremor and earthquakes, *Nat. Geosci.*, *4*, 384–388, doi:10.1038/ngeo1141.

Siegfried, M. R., H. A. Fricker, S. P. Carter, and S. Tulaczyk (2016), Episodic ice velocity fluctuations triggered by a subglacial flood in West Antarctica, *Geophys. Res. Lett.*, *43*, 2640–2648, doi:10.1002/2016GL067758.

Stokes, C. R., M. Margold, C. D. Clark, and L. Tarasov (2016), Ice stream activity scaled to ice sheet volume during Laurentide Ice Sheet deglaciation, *Nature*, *530*, 322–326, doi:10.1038/nature16947.

Terzaghi, K. (1950), Mechanism of landslides, in *Application of Geology to Engineering Practice*, edited by S. Paige, pp. 83–123, Geol. Soc. of Am., New York, doi:10.1130/Berkey.1950.

Thompson, J., M. Simons, and V. C. Tsai (2014), Modeling the elastic transmission of tidal stresses to great distances inland in channelized ice streams, *Cryosphere*, *8*, 2007–2029, doi:10.5194/tc-8-2007-2014.

Tulaczyk, S. (2006), Scale independence of till rheology, *J. Glaciol.*, *52*(178), 377–380, doi:10.3189/172756506781828601.

Tulaczyk, S., W. B. Kamb, and H. F. Engelhardt (2000), Basal mechanics of Ice Stream B, West Antarctica 1. Till mechanics, *J. Geophys. Res.*, *105*, 463–481, doi:10.1029/1999JB900329.

Walker, R. T., B. R. Parizek, R. B. Alley, S. Anandakrishnan, K. L. Riverman, and K. Christianson (2013), Ice-shelf tidal flexure and subglacial pressure variations, *Earth Planet. Sci. Lett.*, *361*, 422–428, doi:10.1016/j.epsl.2012.11.008.

Winberry, J. P., S. Anandakrishnan, D. A. Wiens, R. B. Alley, and K. Christianson (2011), Dynamics of stick–slip motion, Whillans Ice Stream, Antarctica, *Earth Planet. Sci. Lett.*, *305*, 283–289, doi:10.1016/j.epsl.2011.02.052.

Winberry, J. P., S. Anandakrishnan, R. B. Alley, D. A. Wiens, and M. J. Pratt (2014), Tidal pacing, skipped slips and the slowdown of Whillans Ice Stream, Antarctica, *J. Glaciol.*, *60*, 795–807, doi:10.3189/2014JoG14J038.

Yao, M., and A. Anandarajah (2003), Three-dimensional discrete element method of analysis of clays, *J. Eng. Mech.*, *129*, 585–596, doi:10.1061/(ASCE)0733-9399(2003)129:6(585).

Zhang, Y., and C. S. Campbell (1992), The interface between fluid-like and solid-like behavior in two-dimensional granular flows, *J. Fluid Mech.*, *237*, 541–568, doi:10.1017/S0022112092003525.

Zhou, Z. Y., S. B. Kuang, K. W. Chu, and A. B. Yu (2010), Discrete particle simulation of particle-fluid flow: Model formulations and their applicability, *J. Fluid Mech.*, *661*, 482–510, doi:10.1017/S0022112010003063X.